GEOHAZARDS AND ENVIRONMENTAL RISK ASSESSMENT PRACTICES OF PETROLEUM AND GAS PIPELINES USING MICROWAVE REMOTE SENSING

Emil Bayramov[1,2], Manfred Buchroithner[2], Martin Kada[3], Saida Aliyeva[4]

•

[1] Nazarbayev University, Kazakhstan
[2] TU Dresden, Germany
[3] Technical University of Berlin, Germany
[4] ADA University, Azerbaijan
emil.bayramov@nu.edu.kz
manfred.buchroithner@tu-dresden.de
martin.kada@tu-berlin.de
saaliyeva@ada.edu.az

Abstract

These studies focused on the quantitative assessment of the surface displacement velocities and rates and their natural and man-made controlling factors as the potential risks along the seismically active 70 km section of buried oil and gas pipeline in Azerbaijan using Persistent Scatterer Interferometric Synthetic Aperture Radar (PS-InSAR) and Small Baseline Subset (SBAS-InSAR) remote sensing analysis. The diverse spatial distribution and variation of ground movement processes along pipelines demonstrated that general geological and geotechnical understanding of the study area is not sufficient to find and mitigate all the critical sites of subsidence and uplifts for the pipeline operators. This means that both techniques outlined in this paper provide a significant improvement for ground deformation monitoring or can significantly contribute to the assessment of geohazards and preventative countermeasures along petroleum and gas pipelines.

Keywords: PS-InSAR, SBAS-InSAR, remote sensing, geospatial, pipelines, oil and gas, radar, interferometry

I. Introduction

This research focused on the quantitative assessment of the ground deformations, their natural and man-made controlling factors as the potential risks along a 70 km long seismically active section of buried Baku–Tbilisi–Ceyhan Oil (BTC), South Caucasus Gas (SCP), Western Route Oil (WREP) and South Caucasus Pipeline Expansion Gas (SCPX) pipelines in Azerbaijan. In the frame of this research, the primary goal was to measure and map ground deformation velocities and rates along buried oil and gas pipelines over the period of 2017-2019 using PS-InSAR and SBAS-InSAR remote sensing techniques and cross-correlate the results.

The present studies hold the practical scientific value and advantage for the petroleum and gas industry with the focus on pipeline operators, since the prediction, relevant justified investment and mitigation of risks require the combined quantitative and qualitative assessment of actual ground movements and evaluation of potential consequences. Another practical value is the ability to remotely monitor ground movements, reducing the number of expensive, time-

consuming and dangerous field studies (Hole *et al.* 2011).

II. Methods

SBAS-InSAR and PS-InSAR analysis along petroleum and gas pipelines were applied to identify the spatial patterns of ground surface deformations with respect to the location of active seismic faults (Fig.1a-d). The workflow shown in Fig.2 was used for PS-InSAR and SBAS-InSAR techniques, geospatial interpolations and spatial statistical analysis.

The monitoring and characterization of ground deformation processes along the 70 km section of oil and gas pipelines have been carried out by using a stack of total of 59 Sentinel-1 satellite images using PS-InSAR and SBAS-InSAR techniques. Sentinel-1 satellite images were acquired in C-band (wavelength 5.55 cm) with a revisiting time of 6 days considering both satellites (Sentinel-1A and Sentinel-1B) and an achievable ground resolution of 5 m × 20 m (range × azimuth) for the Single Look Complex (SLC) product. The radar images cover the period January 2018 - December 2019 and have been acquired in descending orbit with VV + VH polarizations, IW beam mode, Path-6 and Absolute Orbit-29828. Sentinel-1 VV polarization bands were used since co-polarized bands provide higher coherency (Imamoglu *et al.* 2019). As it is possible to observe in Figure 3a-d, all images are well connected in time for the interferometric analysis.

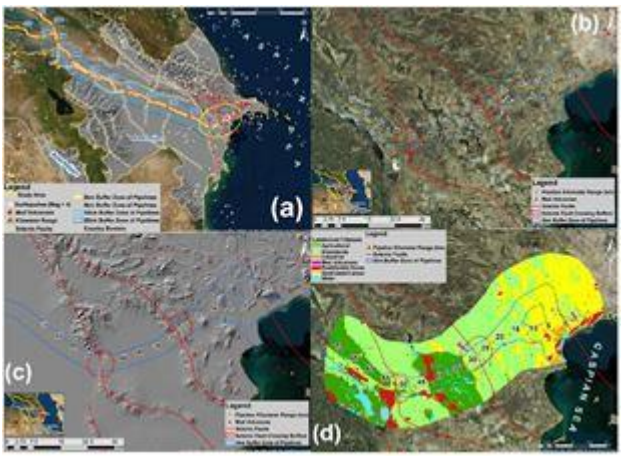

Fig. 1: *(a) Map of Corridors of Oil and Gas Pipelines with the Indication of Seismic Faults, Earthquakes, Mud Volcanoes; (b) Detailed Map of Study Area with the Worldview-2 Satellite Imagery Background; (c) Detailed Map of Study Areas with the Hillshaded Terrain Background; (d) Landcover Types along the Corridor of Oil and Gas Pipelines.*

PS-InSAR is a proven differential interferometric technique which involves processing of multi-temporal Synthetic Aperture Radar (SAR) data to identify persistently scattering ground features and their motion rates with millimetre precision (Ferretti *et al.* 2011).

The SBAS interferometric technique is based on the generation of interferograms through the processing of small spatial and temporal baseline interferometric pairs in order to reduce decorrelation and topographic effects (Berardino *et al.* 2003).

The main processing steps of PS-InSAR consist of interferogram generation, multi-temporal persistent scatterers (PS-InSAR) processing and removal of atmospheric phase screen (Osmanoglu *et al.* 2016). The main processing steps of SBAS consist of differential interferogram generation from selected SAR image pairs with a small orbital separation (baseline) to reduce the spatial decorrelation and topographic effects, filtering of atmospheric artifacts based on the availability of both spatial and temporal information and removal of topographic phase contribution (Lauknes *et al.* 2005).

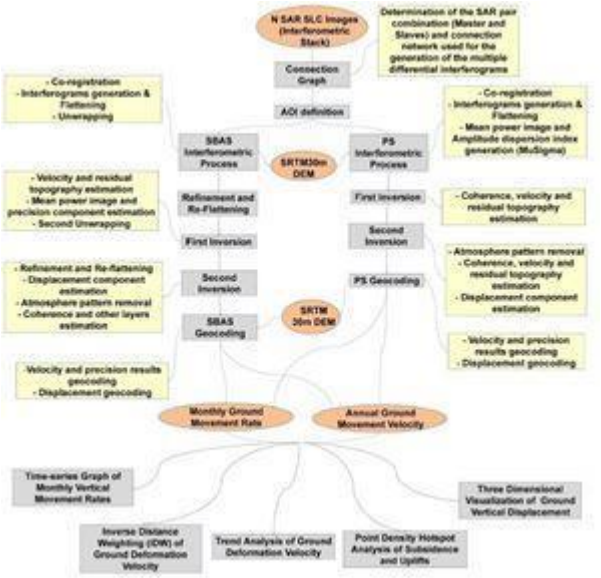

Fig. 2: *Workflow for PS-InSAR, SBAS-InSAR and Spatial Statistics*

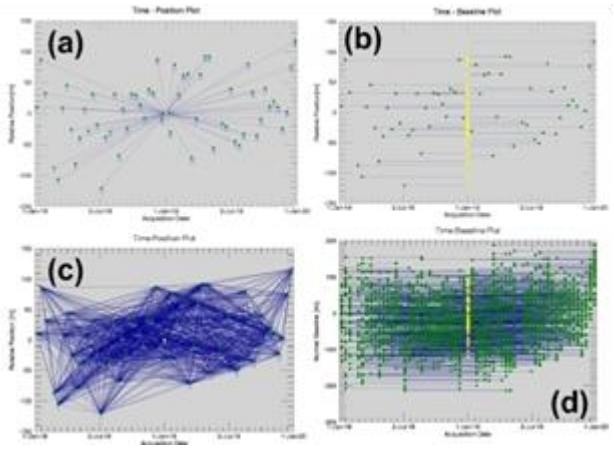

Fig. 3: *Connection Graphs: (a) Time-Position Plot for PS-InSAR; (b) Time-Baseline Plot for PS-InSAR; (c) Time-Position for SBAS-InSAR; (d) Time-Baseline Plot for SBAS-InSAR;*

III. Results and Discussions

As a primary factor of ground deformations, the influence of tectonic movements was observed in the wide scale analysis along 70 km long and 10 km wide section of petroleum and gas pipelines with the prevailing and continuous subsidence in the KP13–70 range of pipelines crossing two active seismic faults (Fig.4a-f; Fig.5a-d; Fig.6a-d). However, the largest subsidence rates were observed in the areas of croplands, where agricultural activities, such as overuse of groundwater, irrigation and ploughing etc. accelerate the surface deformation rates caused by the tectonic processes. The ground uplift deformations were observed in the pipeline range of KP0-KP13.

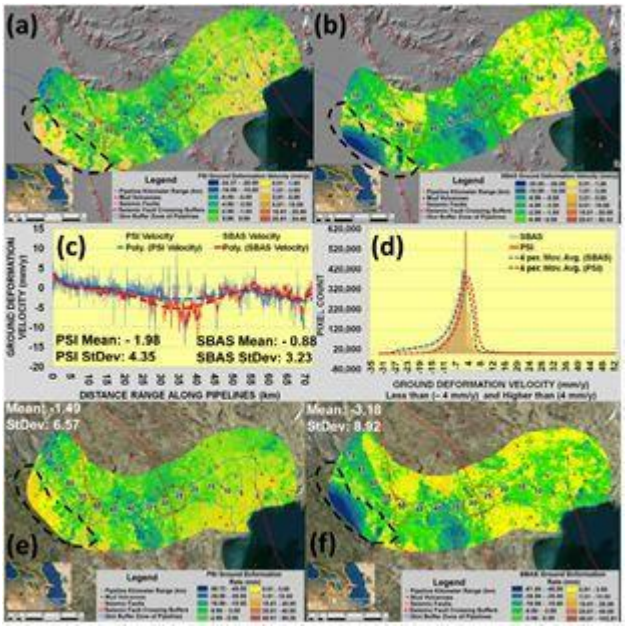

Fig. 4: *(a) Map of PS-InSAR Ground Deformation Velocity along Petroleum and Gas Pipelines; (b) Map of SBAS-InSAR Ground Deformation Velocity along Petroleum and Gas Pipelines; (c) PS-InSAR and SBAS-InSAR 5km Interval Profile View of Ground Deformation Velocity; (d) Histogram of PS-InSAR and SBAS-InSAR Pixel Distribution; (e) PS-InSAR Map of Ground Movement Rates (on 27 December 2019 with the Baseline of 6 January 2018); (f) SBAS-InSAR Map of Ground Movement Rates (on 27 December 2019 with the Baseline of 6 January 2018).*

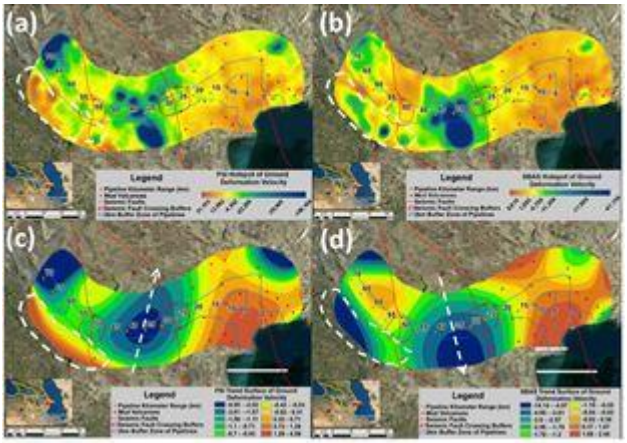

Fig. 5: *(a) Map of PS-InSAR Hotspots of Ground Deformation Velocities; (b) Map of SBAS-InSAR Hotspots of Ground Deformation Velocities; (c) Map of PS-InSAR Trends of Ground Deformation Velocities; (d) Map of SBAS-InSAR Trends of Ground Deformation Velocities.*

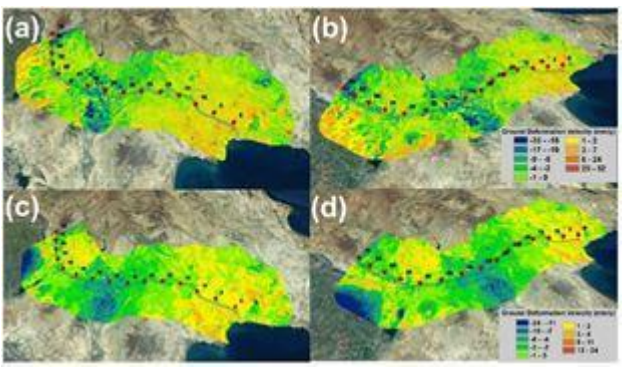

Fig. 6: *Three-Dimensional Representation of PS-InSAR and SBAS-InSAR Ground Deformation Velocities (Visual Exaggeration: 3 times): (a) PS-InSAR South-West View; (b) PS-InSAR South-East View; (c) SBAS-InSAR South-West View; (d) SBAS-InSAR South-East View.*

SBAS-InSAR performed better than PS-InSAR along buried petroleum and gas pipelines in the following aspects: the complete coverage of the measured points (Fig.7a-b), significantly lower dispersion of the results, continuous and realistic measurements and higher accuracy of ground deformation rates against the GPS historical measurements.

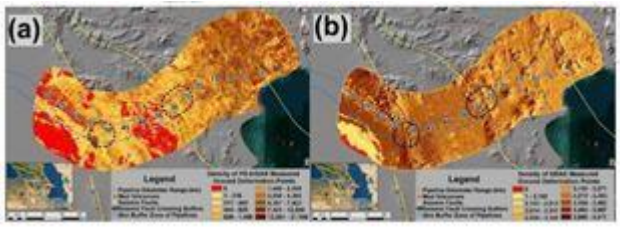

Fig. 7: *(a) Density of PS-InSAR Measured Ground Deformation Points; (b) Density of SBAS-InSAR Measured Ground Deformation*

The validation of ground deformation rates at KP28 + 300 using high-precision GPS measurements revealed the encouraging level of agreement with the regression coefficients equal to 0.94 for SBAS-InSAR and 0.74 for PS-InSAR (Fig. 8a-d). The validation of ground deformation rates at KP52 + 500 using high-precision GPS measurements revealed the encouraging level of agreement with the regression coefficients equal to 0.9 for SBAS-InSAR and 0.89 for PS-InSAR (Fig.8a-d). This means that the SBAS-based approach outlined in this paper is a significant improvement over current ground-based monitoring practices along pipelines. However, it is necessary to emphasize that PS-InSAR could perform better for the terminals, pump stations and aboveground pipelines since the PS-InSAR technique relies on the intensity of the backscattered radar waves to measure permanent scatterers as man-made structures with strongest returns.

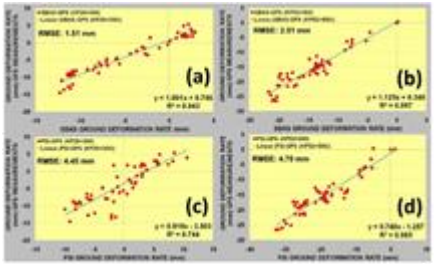

Fig. 8: *(a) Validation of SBAS-InSAR Ground Deformation Rates using High-precision GPS Measurements at KP28 + 300; (b) Validation of SBAS-InSAR Ground Deformation Rates using High-precision GPS Measurements at KP52 + 500; (c) Validation of PS-InSAR Ground Deformation Rates using High-precision GPS Measurements at KP28 + 300; (d) Validation of PS-InSAR Ground Deformation Rates using High-precision GPS Measurements at KP52 + 500.*

Local scale analyses were performed along 70 km section of pipelines with 250 m buffer zone for the detailed quantitative ground movement assessment of two seismic faults. Although both PS-InSAR and SBAS-InSAR measurements were highly consistent in deformation patterns and trends along pipelines, they showed differences in the spatial distribution of ground deformation classes and noisiness of produced results.

High dispersion of PS-InSAR measurements caused low regression coefficients with SBAS-InSAR for the pipeline profile range of 70 km and seismic faults at KP21–31 and KP46–54.

The minimum and maximum vertical ground deformation velocities were observed to be −21.3 and 14.1 mm/y for PS-InSAR and −15.9 and 4.5 mm/y for SBAS-InSAR measurements, respectively, along a 70 km range of pipelines with the buffer zone of 250m (Fig.9a-d).

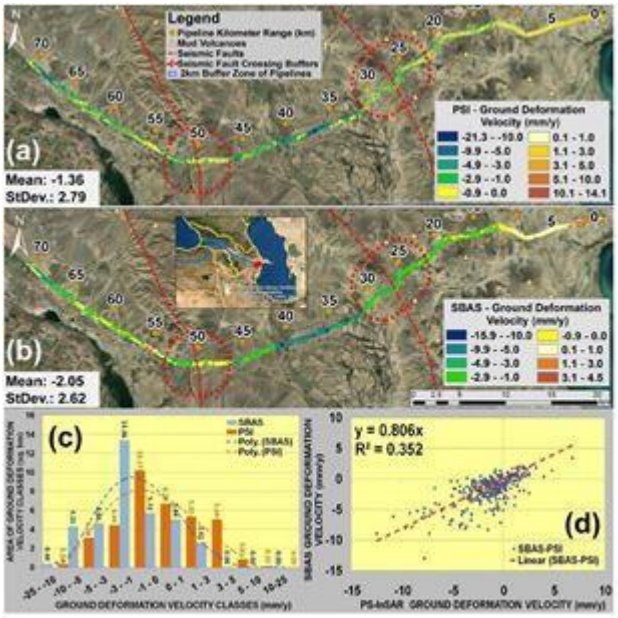

Fig. 9: *Map of Ground Deformation Velocity along 70 km Petroleum and Gas Pipelines Corridor within 250 m Buffer Zone; (a) for PS-InSAR; (b) for SBAS-InSAR; (c) Area of Ground Deformation Velocity Classes; (d) Regression Analysis between PS-InSAR and SBAS-InSAR Ground Deformation Velocity for 250 m Interval Points along Pipelines.*

The minimum and maximum vertical ground deformation rates were observed to be −41.3 and 32.6 mm for PS-InSAR and −28.2 and 8.2 mm for SBAS-InSAR measurements, respectively, along a 70 km range of pipelines with the buffer zone of 250m (Fig.10a-d).

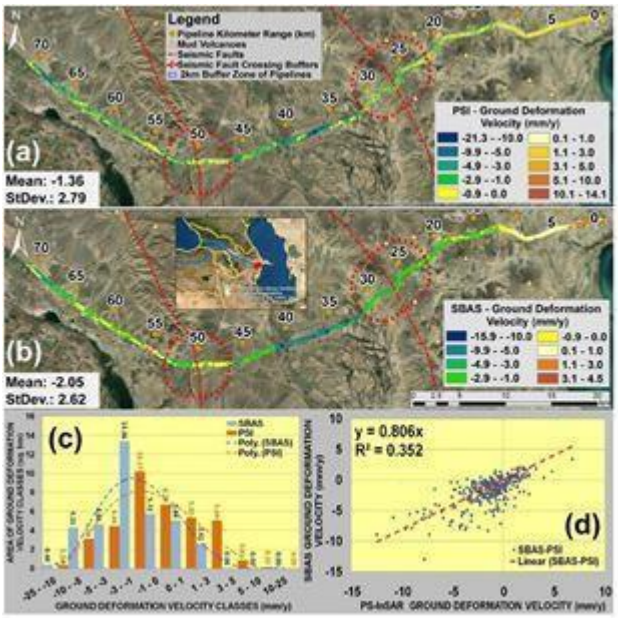

Fig. 10: *Map of Ground Deformation Rates along 70 km Petroleum and Gas Pipelines Corridor within 250 m Buffer Zone; (a) for PS-InSAR; (b) for SBAS-InSAR; (c) Area of Ground Deformation Rate Classes; (d) Regression Analysis between PS-InSAR and SBAS-InSAR Ground Deformation Rates for 250 m Interval Points along Pipelines.*

The ground deformation velocities within the range of Seismic Fault KP21–31 revealed the minimum and maximum values of −9.03 and 1.45 mm/y for SBAS-InSAR and −22.65 and 14.01 mm/y for PS-InSAR, respectively (Fig.11a-d).

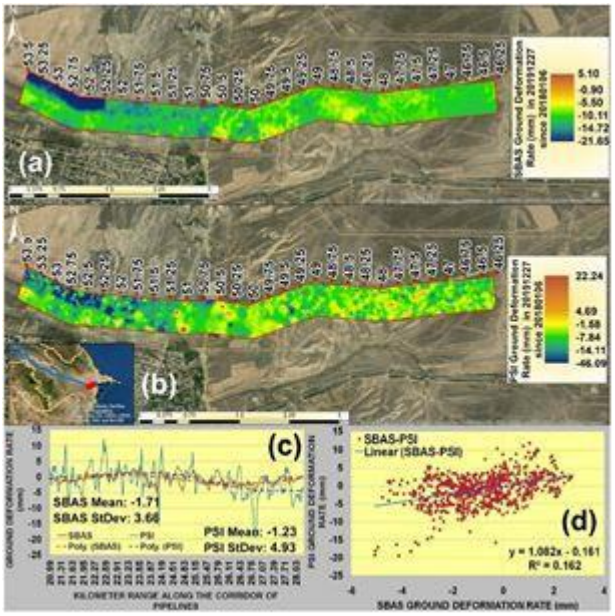

Fig. 11: *Detailed Map of the Ground Deformation Velocity for 250 m Buffer Zone of Pipeline Corridor Crossing the Seismic Faults at KP21–31 range: (a) for SBAS-InSAR; (b) for PS-InSAR;(c) Profile View of PS-InSAR and SBAS-InSAR Ground Deformation Velocity for the Seismic Fault at KP21–31 range; (d) Regression Analysis between PS-InSAR and SBAS-InSAR Ground Deformation Velocity for 10m Interval Points along Pipelines within KP21–31 range.*

The ground deformation rates within the range of Seismic Fault KP21–31 revealed the minimum and maximum values of −12.24 and 8.23 mm for SBAS-InSAR and −46.07 and 33.46 mm for PS-InSAR, respectively (Fig.12a-d).

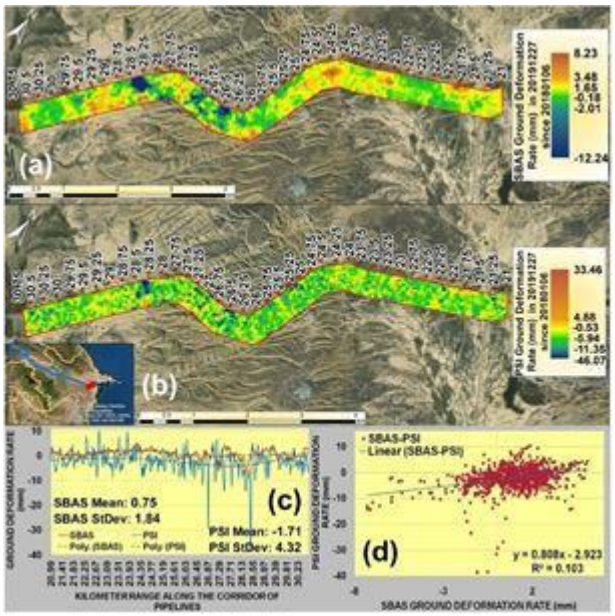

Fig. 12: *Detailed Map of the Ground Deformation Rates for 250 m Buffer Zone of Pipeline Corridor Crossing the Seismic Faults at KP21–31 Range: (a) for SBAS-InSAR; (b) for PS-InSAR; (c) Profile View of PS-InSAR and SBAS-InSAR Ground Deformation Rates for the Seismic Fault at KP21–31 Range; (d) Regression Analysis between PS-InSAR and SBAS-InSAR Ground Deformation Rates for 10m Interval Points along Pipelines within KP21–31 Range.*

The ground deformation velocities within the range of Seismic Fault KP46–54 revealed the minimum and maximum values of −8.31 and 2.05 mm/y for SBAS-InSAR and −19.14 and 9.41 mm/y for PS-InSAR, respectively (Fig.13a-d).

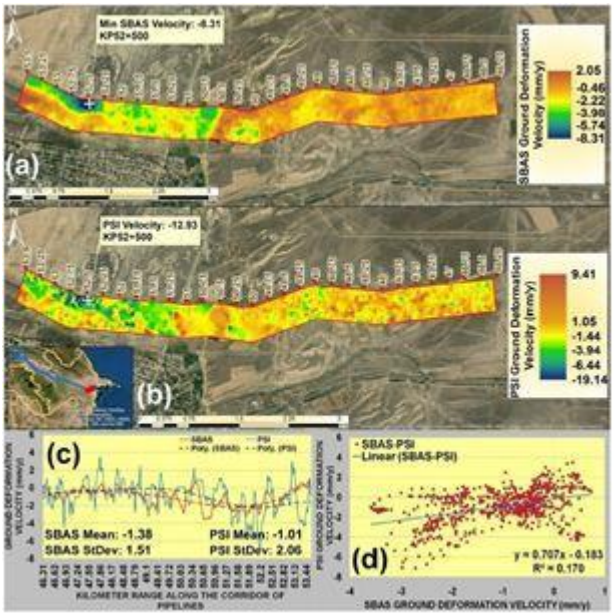

Fig. 13: *Detailed Map of the Ground Deformation Velocity for 250 m Buffer Zone of Pipeline Corridor Crossing the Seismic Faults at KP46–54 range: (a) for SBAS-InSAR; (b) for PS-InSAR; (c) Profile View of PS-InSAR and SBAS-InSAR Ground Deformation Velocity for the Seismic Fault at KP46–54 range; (d) Regression Analysis between PS-InSAR and SBAS-InSAR Ground Deformation Velocity for 10m Interval Points along Pipelines within KP46–54 Range.*

The ground deformation rates within the range of Seismic Fault KP46–54 revealed the minimum and maximum values of −21.65 and 5.1 mm for SBAS-InSAR and −46.09 and 22.24 mm for PS-InSAR, respectively (Fig.14a-d).

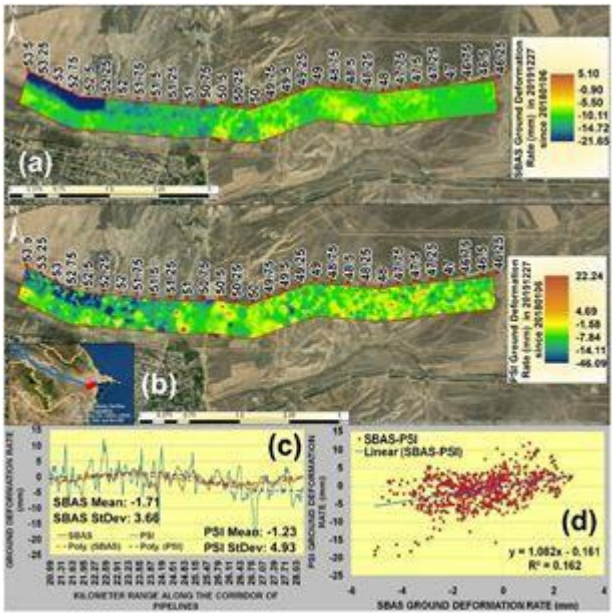

Fig. 14: *Detailed Map of the Ground Deformation Rates for 250 m Buffer Zone of Pipeline Corridor Crossing the Seismic Faults at KP46–54 Range: (a) for SBAS-InSAR; (b) for PS-InSAR; (c) Profile View of PS-InSAR and SBAS-InSAR Ground Deformation Rates for the Seismic Fault at KP46–54 range; (d) Regression Analysis between PS-InSAR and SBAS-InSAR Ground Deformation Rates for 10m Interval Points along Pipelines within KP46–54 range.*

The wider range of PS-InSAR values was directly related to the produced dispersion results, which makes it more complicated for the pipeline operators to prioritize vulnerable areas to ground deformation processes along pipelines.

The regression analysis and RMSE evaluations between SBAS-InSAR and PS-InSAR ground

deformation measurements revealed the correlation coefficient equal to 0.79 and RMSE equal to 4.9 mm for KP28 + 300 and the correlation coefficient equal to 0.92 and RMSE equal to 6 mm for KP52 + 500. This allows us to assume that SBAS-InSAR and PS-InSAR measurements are subject to approximate variations in the range of 4.9–6 mm, which should be considered as a limitation by pipeline operators in terms of the existing compliance standards for acceptance (Fig.15a-d).

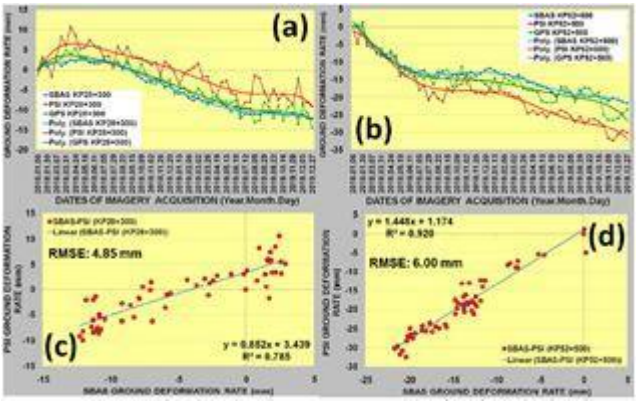

Fig. 15: *(a) Graph of Ground Deformation Rates for SBAS, PS-InSAR and GPS Measurements at KP28 + 300; (b) Graph of Ground Deformation Rates for SBAS-InSAR, PS-InSAR and GPS Measurements at KP52 + 500; (c) Regression Analyses between SBAS-InSAR and PS-InSAR Ground Deformation Rates at KP28 + 300; (d) Regression Analyses between SBAS-InSAR and PS-InSAR Ground Deformation Rates at KP52 + 500.*

The spatial distribution and variation of ground movement processes along pipelines demonstrated that general geological and geotechnical understanding of the study area is not sufficient to find and mitigate all the critical areas of subsidence and uplifts for the pipeline operators. The prediction of the potential subsidence or uplift locations based on the field visual verifications holds a lot of uncertainties without wide and detailed scale airborne and satellite space observation technologies. The justification of the budget for the geotechnical maintenance activities along long-range oil and gas pipelines requires sophisticated prioritization and planning of the remediation sites and clear quantitative and qualitative risk assessment proving the activeness of these sites and effectiveness of the remediation measures.

Even though SBAS-InSAR demonstrated a reliable approach for the detection of ground deformation processes along petroleum and gas pipelines, it is highly recommended to advance these studies with the integration of other geological, geotechnical, thermal and climatic information to better understand controlling natural and man-made factors.

IV. Conclusions

Both SBAS-InSAR and PS-InSAR techniques showed that the continuous subsidence was prevailing in the kilometer range of 13-70 of oil and gas pipelines crossing two seismic faults. The ground uplift deformations were observed in the pipeline kilometer range of 0-13. Although both PS-InSAR and SBAS-InSAR measurements were highly consistent in deformation patterns and trends along pipelines, they showed differences in the spatial distribution of ground deformation classes and noisiness of produced results. High dispersion of PS-InSAR measurements caused low regression coefficients with SBAS-InSAR for the entire pipeline kilometer range of 0-70. SBAS-InSAR showed better performance than PS-InSAR along buried petroleum and gas pipelines in the following aspects: the complete coverage of the measured points, significantly lower dispersion of the results, continuous and realistic measurements and higher accuracy of ground deformation rates against the GPS historical measurements. As a primary factor of ground deformations, the influence of tectonic movements was observed in the wide scale analysis along 70 km long and 10 km wide section of petroleum and gas pipelines; however, the largest subsidence rates were observed in the areas of agricultural activities which accelerate the deformation rates caused by

the tectonic processes. The diverse spatial distribution and variation of ground movement processes along pipelines demonstrated that general geological and geotechnical understanding of the study area is not sufficient to find and mitigate all the critical sites of subsidence and uplifts for the pipeline operators. This means that both techniques outlined in this paper provide a significant improvement for ground deformation monitoring or can significantly contribute to the assessment of geohazards and preventative countermeasures along petroleum and gas pipelines.

Acknowledgements and Funding. The authors would like to thank Nazarbayev University. This research was funded by the Nazarbayev University through the Social Policy Grant and the Faculty-development Competitive Research Grant (FDCRGP) - Funder Project Reference: 080420FD1917.

References

[1] Berardino, P., Costantini, M., Franceschetti, G., Iodice, A., Pietranera, L., Rizzo, V. (2003). Use of differential SAR interferometry in monitoring and modelling large slope instability at Maratea (Basilicata, Italy). Eng. Geol. 2003, 68, 31–51.

[2] Hole, J., Holley, R., Giunta, G., Lorenzo, G., Thomas, A. InSAR assessment of pipeline stability using compact active transponders. In Proceedings of the Fringe 2011, Frascati, Italy, 19–23 September 2011; p. 53.

[3] Imamoglu, M., Kahraman, F., Çakir, Z., Sanli, F.B. 2019. Ground Deformation Analysis of Bolvadin (W. Turkey) by Means of Multi-Temporal InSAR Techniques and Sentinel-1 Data. Remote Sens., 11, 1069.

[4] Lauknes, T.R., Dehls, J., Larsen, Y., Høgda, K.A., Weydahl, D.J. (2005). A comparison of SBAS and PS ERS InSAR for subsidence monitoring in Oslo, Norway. In Proceedings of the Fringe 2005 Workshop, ESA ESRIN, Frascati, Italy, 28 November–2 December 2005.

[5] Ferretti, A., Fumagalli, A., Novali, F., Prati, C.; Rocca, F., Rucci, A. (2011). A New Algorithm for Processing Interferometric Data-Stacks: SqueeSAR. IEEE Trans. Geosci. Remote Sens. 49, 3460–3470.

[6] Osmanoglu, B.; Sunar, F.; Wdowinski, S.; Cabral-Cano, E. (2016). Time series analysis of InSAR data: Methods and trends. ISPRS J. Photogramm. Remote Sens., 115, 90–102.